Optical Materials 33 (2011) 1514–1518

Contents lists available at ScienceDirect

Optical Materials

journal homepage: www.elsevier.com/locate/optmat

Luminescence quenching processes in $Gd_2O_2S:Pr^{3+},Ce^{3+}$ scintillating ceramics

Samuel Blahuta [a,b,*], Bruno Viana [a], Aurélie Bessière [a], Eric Mattmann [b], Brian LaCourse [b]

[a] Laboratoire de Chimie de la Matière Condensée de Paris, UMR – CNRS 7574, Chimie-Paristech, 11 rue Pierre et Marie Curie, 75231 Paris Cedex 05, France
[b] Saint-Gobain Cristaux et Détecteurs, 104 Route de Larchant, 77140 St-Pierre-lès-Nemours, France

ARTICLE INFO

Article history:
Received 15 October 2010
Received in revised form 21 February 2011
Accepted 28 February 2011
Available online 23 March 2011

Keywords:
Scintillator
Ceramic
Luminescence quenching
Electronic defects

ABSTRACT

Temperature dependent radioluminescence under X-ray excitation (XRL) and luminescence decay time measurements following 430 nm laser excitation have been performed in the 10–775 K range on $Gd_2O_2S:Pr^{3+},Ce^{3+}$ scintillating ceramics. From 200 K to both low and high temperature, XRL light yield decreases by 60%. High temperature luminescence quenching has been revisited. Temperature dependent lifetime measurements imply non-radiative de-excitation mechanism at electronic defects spatially correlated to Pr^{3+} emitting ions. At low temperatures, decreasing XRL light yield with irradiation time is linked to very intense thermoluminescence (TL) peak around 120 K ascribed to sulfur vacancies. These traps cause efficient electron trapping which competes with the prompt recombination mechanism.

1. Introduction

The rapid development of medical imaging equipment such as X-ray computed tomography (X-ray CT), has increased the need for highly efficient X-ray detectors. The scintillating materials required for X-ray CT should have high X-ray absorption efficiency, high light yield, low residual luminescence (afterglow), and good spectral match to photodiode sensitivity for photoelectric conversion [1]. Gadolinium oxysulfide (Gd_2O_2S) is currently used as an efficient host to make scintillation materials for medical imaging applications because its high density (7.34 g/cm^3) and high atomic number ($Z = 64$) of Gd [2,3] lead to high X-ray stopping power. When doped with Pr^{3+} the resulting scintillator shows light yield up to 50,000 photons/MeV [1] and relatively low afterglow [4,5]. Ce^{3+} is also frequently added as a co-doping element because it efficiently reduces the afterglow of $Gd_2O_2S:Pr^{3+}$ and $Gd_2O_2S:Tb^{3+}$ phosphors [6]. Ce^{3+} is also supposed to increase the resistance to radiation damage [7]. Thus, $Gd_2O_2S:Pr^{3+},Ce^{3+}$ can be used as an efficient scintillator for X-ray tomography.

Gadolinium oxysulfide has a hexagonal lattice (space group $P\bar{3}m1$ and lattice parameters $a = 3.851$ Å and $c = 6.664$ Å) showing a trigonal symmetry. Due to its non-cubic structure, Gd_2O_2S is mainly found as translucent ceramics. Most of the time, Gd_2O_2S ceramics are fabricated by hot pressing (HP) under vacuum or hot isostatic pressing (HIP) under neutral atmosphere at 1100 °C–1600 °C [2,5–8]. These processing conditions are often very reducing and can lead to the formation of vacancies (either anionic or cationic) which may behave as charge carrier traps and lead to afterglow when thermally emptied [8,9]. In order to understand the luminescence mechanisms in this scintillator, the temperature dependence of several optical and scintillation properties has been investigated. This work continues our previous investigations on new scintillators for imaging equipment [10–13].

2. Experimental

$Gd_2O_2S:Pr,Ce$ ceramics were provided by Saint-Gobain Crystals and Detectors. The powders used to prepare ceramics are commercially available and contained 700 at ppm Pr. Glow Discharge Mass Spectrometry analysis confirmed that no impurity was present in a significant amount. 10 at ppm Cerium was then added as Ce_2O_3. X-ray diffraction on these powders revealed pure phase with space group $P\bar{3}m1$. The process includes HP and HIP as can be found in the literature [2,5–8]. For confidentiality matters details (temperature, atmosphere) cannot be further described but are not relevant parameters for this study. Materials greater than 99% dense were thus obtained. Scanning electron microscopy revealed anisotropically shaped grains with sizes ranging from 10 to 70 μm. The small amount of porosity that was observed was mainly inter-granular with diameter less than 1 μm.

TL measurements were performed on a $10 \times 10 \times 1$ mm^3 ceramic. The sample was glued with silver paint to a copper sample holder attached to the cold head of a Janis cryostat and placed under vacuum. The sample was first excited *in situ* at 10 K for 10 min by a molybdenum X-ray source operating at 50 kV and 20 mA. The excitation beam goes through a Beryllium window in the cryostat

* Corresponding author at: Laboratoire de Chimie de la Matière Condensée de Paris, UMR – CNRS 7574, Chimie-Paristech, 11 rue Pierre et Marie Curie, 75231 Paris Cedex 05, France. Tel.: +33 1 53 73 79 39; fax: +33 1 46 34 74 89.
E-mail address: samuel-blahuta@chimie-paristech.fr (S. Blahuta).

0925-3467/$ - see front matter © 2011 Elsevier B.V. All rights reserved.
doi:10.1016/j.optmat.2011.02.040

and hits the sample surface at a 45° angle. The sample was heated at 20 K/min between 10 K and 650 K using a LakeShore 340 temperature controller.

Luminescence was collected *via* an optical fiber by a Princeton CCD camera cooled to −65 °C coupled with an Acton SpectraPro 1250i monochromator equipped with a grating to allow spectral resolution. The emitted light was collected from the irradiated side of the ceramics at 45° to the sample surface.

The same equipment was used for measuring radioluminescence under X-ray excitation at various temperatures. Radioluminescence was measured every 50 K from 650 K to 10 K. The CCD camera shutter aperture was set to 1s, allowing good signal to noise ratio. Relative light outputs are calculated by integrating the background subtracted emission spectrum.

Fluorescence spectra and luminescence decay times were also measured. The excitation source was an optical parametric oscillator laser (10 Hz, 8 ns) pumped by the third harmonic of a YAG:Nd laser and operating at 430 nm. A Roper/Princeton ICCD detector was used to detect the fluorescence with a time delay up to 50 μs. The ceramic samples were silver-glued to a copper sample holder. For the 300 K to 800 K measurements, the sample holder was mounted on the top of a heating element. For the low temperature measurements, the sample was mounted on the cold head of a closed cycle cryogenic refrigerator.

3. Results

XRL measurements were carried out on a $Gd_2O_2S:Pr^{3+},Ce^{3+}$ ceramic from high to low temperature (from 650 K to 10 K) in order to avoid any possible contribution from thermally released charge carriers to the luminescence [14]. The emission spectra at 650 K, 300 K and 10 K are shown in Fig. 1. For comparison, all spectra have been normalized. Due to the localization of Pr^{3+} 5*d* energy levels in the conduction band of the Gd_2O_2S host lattice [15], no $4f5d$–$4f^2$ emission is observed. The spectra are composed entirely of Pr^{3+} $4f^2$–$4f^2$ lines. At 10 K and room temperature (RT), the emission spectrum mainly shows the Pr^{3+} $^3P_{i\ (i=0,1,2)} \rightarrow {}^3F_{j\ (j=2,3,4)}$, $^3H_{k\ (k=4,5,6)}$ $4f^2$–$4f^2$ transitions. In particular, $^3P_0 \rightarrow {}^3H_4$ peaks at 514 nm and $^3P_0 \rightarrow {}^3F_2$ at 667 nm [16]. With increasing temperature, the emission bands broaden due to thermal effects and new bands appear. A new broad peak appears around 630 nm at 650 K which corresponds to $^1D_2 \rightarrow {}^3H_j$ transitions. This emission is also present at RT but only constitutes 1–2% of the total spectrum [17]. This point will be further discussed later. As shown in Fig. 1, two energy levels, $^3P_0$ and $^1D_2$ are responsible for almost the whole emission spectrum. Note that when the temperature increases, $^3P_1$ and $^3P_2$ levels also contribute to the luminescence, as they are thermally populated via $^3P_0$.

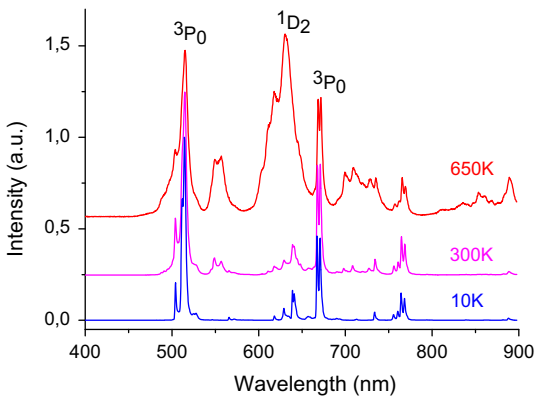

Fig. 1. XRL spectra of $Gd_2O_2S:Pr^{3+},Ce^{3+}$ at 650 K, 300 K and 10 K. All spectra have been normalized and are only composed of Pr^{3+} $4f^2$–$4f^2$ lines.

For each measurement (every 50 K from 650 K to 10 K), the area under the 400–900 nm spectrum has been calculated and is plotted as a function of temperature in Fig. 2a. Two parts can be distinguished in the evolution of the total intensity over the visible spectrum with temperature. From 200 K to 10 K, a 60% decrease of the 200 K luminescence intensity is observed. The 200–650 K range shows a 58% decrease of the 200 K luminescence intensity with increasing temperature. Similar low and high temperature luminescence quenching have been observed by Drozdowski et al. on Pr-doped LuAG [14], but it was mainly concerning $4f5d$–$4f^2$ luminescence of Pr^{3+}. Nevertheless radioluminescence decrease of about 50% is reported for the $4f^2$–$4f^2$ emission above 175 K in their work but no low temperature quenching was observed. Temperature quenching of Gd_2O_2S:Pr,Ce luminescence was also reported by Blasse and Meijerink, but only above 300 K [17]. As will be discussed later on, this work at lower temperature allows us to bring new insights to the luminescence mechanism.

Fig. 2b shows the evolution of the maximum of the $^3P_0 \rightarrow {}^3H_4$ and the $^1D_2 \rightarrow {}^3H_4$ emissions at 514 nm and 630 nm respectively. The $^3P_0 \rightarrow {}^3H_4$ emission shows a similar evolution with temperature to the total intensity evolution shown in Fig. 2a. Indeed the emission corresponding to transitions from the $^1D_2$ level is only 1–2% of the total emission at 300 K, and can hardly be seen at lower temperatures. When the temperature increases, the $^1D_2 \rightarrow {}^3H_4$ emission increases steadily and at 650 K it is 2 times greater than the emission at 10 K. This emission presents lower amplitude than the $^3P_0 \rightarrow {}^3H_4$ line, except at 650 K where both emissions have the same peak intensity, as can be seen in Fig. 1. As a consequence, the total emission intensity of this scintillator under X-ray excitation is

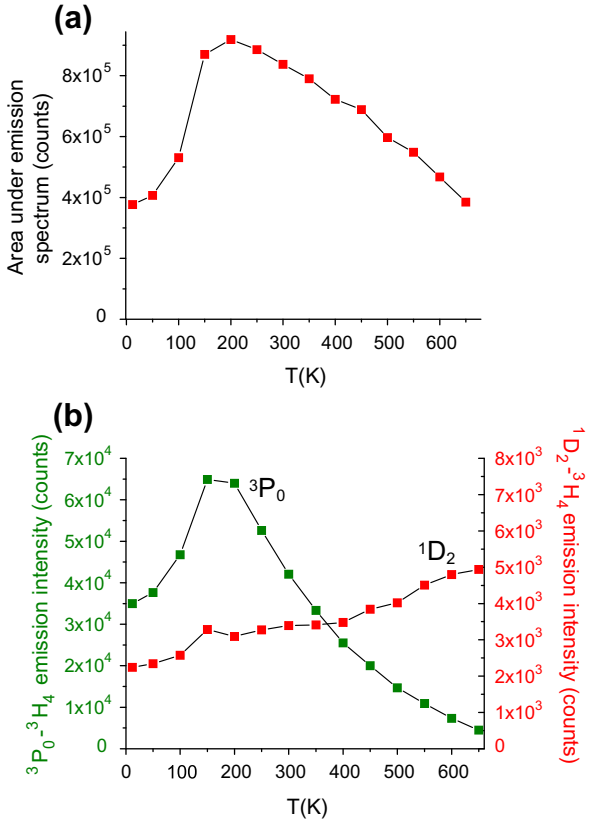

Fig. 2. Evolution with temperature of (a) the total luminescence intensity (area under the XRL spectra over the 400–900 nm region); (b) the intensity of the $^3P_0 \rightarrow {}^3H_4$ and $^1D_2 \rightarrow {}^3H_4$ emissions at 514 nm and 630 nm respectively.